A genome-scale metabolic network of the aroma bacterium Leuconostoc mesenteroides subsp. cremoris

Özcan, Emrah; Selvi, S. Selvin; Nikerel, Emrah; Teusink, Bas; Toksoy Öner, Ebru; Çakr, Tunahan

Link to publication in VU Research Portal

APPLIED MICROBIAL AND CELL PHYSIOLOGY

CrossMark

A genome-scale metabolic network of the aroma bacterium *Leuconostoc mesenteroides* subsp. *cremoris*

Emrah Özcan [1,2,3] · S. Selvin Selvi [2] · Emrah Nikerel [4] · Bas Teusink [3] · Ebru Toksoy Öner [2] · Tunahan Çakır [1]

Abstract

Leuconostoc mesenteroides subsp. *cremoris* is an obligate heterolactic fermentative lactic acid bacterium that is mostly used in industrial dairy fermentations. The phosphoketolase pathway (PKP) is a unique feature of the obligate heterolactic fermentation, which leads to the production of lactate, ethanol, and/or acetate, and the final product profile of PKP highly depends on the energetics and redox state of the organism. Another characteristic of the *L. mesenteroides* subsp. *cremoris* is the production of aroma compounds in dairy fermentation, such as in cheese production, through the utilization of citrate. Considering its importance in dairy fermentation, a detailed metabolic characterization of the organism is necessary for its more efficient use in the industry. To this aim, a genome-scale metabolic model of dairy-origin *L. mesenteroides* subsp. *cremoris* ATCC 19254 (iLM.c559) was reconstructed to explain the energetics and redox state mechanisms of the organism in full detail. The model includes 559 genes governing 1088 reactions between 1129 metabolites, and the reactions cover citrate utilization and citrate-related flavor metabolism. The model was validated by simulating co-metabolism of glucose and citrate and comparing the in silico results to our experimental results. Model simulations further showed that, in co-metabolism of citrate and glucose, no flavor compounds were produced when citrate could stimulate the formation of biomass. Significant amounts of flavor metabolites (e.g., diacetyl and acetoin) were only produced when citrate could not enhance growth, which suggests that flavor formation only occurs under carbon and ATP excess. The effects of aerobic conditions and different carbon sources on product profiles and growth were also investigated using the reconstructed model. The analyses provided further insights for the growth stimulation and flavor formation mechanisms of the organism.

Keywords Lactic acid bacteria · *Leuconostoc mesenteroides* subsp. *cremoris* · Heterolactic fermentation · Flavor metabolism · Genome-scale metabolic model · Flux balance analysis

✉ Tunahan Çakır
tcakir@gtu.edu.tr

1 Department of Bioengineering, Gebze Technical University, Gebze, Kocaeli, Turkey

2 IBSB, Department of Bioengineering, Marmara University, Istanbul, Turkey

3 Systems Bioinformatics, Amsterdam Institute for Molecules, Medicines and Systems, VU Amsterdam, Amsterdam, The Netherlands

4 Genetics and Bioengineering Department, Yeditepe University, Istanbul, Turkey

Introduction

Leuconostoc mesenteroides is a gram-positive, facultative anaerobic lactic acid bacterium used as a member of starter cultures or as a natural inoculum in many fermented foods such as sauerkraut, kimchi, wine, kefir, and cheese (Campedelli et al. 2015; Garvie 1986; Guzel-Seydim et al. 2011). Since the microorganism is responsible for producing significant flavor compounds such as diacetyl and acetoin in dairy products (Hemme and Foucaud-Scheunemann 2004; LevataJovanovic and Sandine 1996; Schmitt et al. 1992), it is an important member of mesophilic cheese starter cultures (Smid et al. 2014). Due to this property, this lactic acid bacterium is referred to as "the aroma bacterium" (Starrenburg and Hugenholtz 1991). *L. mesenteroides* is also recognized as a probiotic microorganism (Yi et al. 2017).

Unlike most lactic acid bacteria (LAB) such as *Lactococcus lactis* or *Lactobacillus plantarum*, *L. mesenteroides* exhibits obligate heterolactic fermentation. It therefore produces significant amounts of CO_2 and ethanol or/and acetate, in addition to lactate (de Paula et al. 2015; Gunsalus and Gibbs 1952). CO_2 production by *L. mesenteroides* leads to "eye formation" in some cheese types (Smid et al. 2014). In homolactic fermentation through the Embden-Meyerhof-Parnas (EMP) pathway, 1 mol of glucose is broken down into 2 mol of lactate, leading to the production of 2 mol of ATP (Ganzle 2015; Gaspar et al. 2013). In obligate heterolactic fermentation, however, 1 mol of lactate is produced per

1 mol of glucose via the phosphoketolase pathway (PKP), which yields only one ATP per glucose (Fig. 1). The glucose is first converted to CO_2 and a C5 and subsequently split by the phosphoketolase enzyme, from which the name PKP is derived, leading to two downstream branches. The branch ending up in lactate production acts as ATP production source for the cell. Under anaerobic conditions, the other branch ends up in ethanol, which acts as redox balance. Under cases of alternative electron sinks, such as aerobic conditions (Plihon et al. 1995) and co-metabolism of citrate (Schmitt and Divies 1992), ethanol can be substituted by acetate, which yields extra ATP.
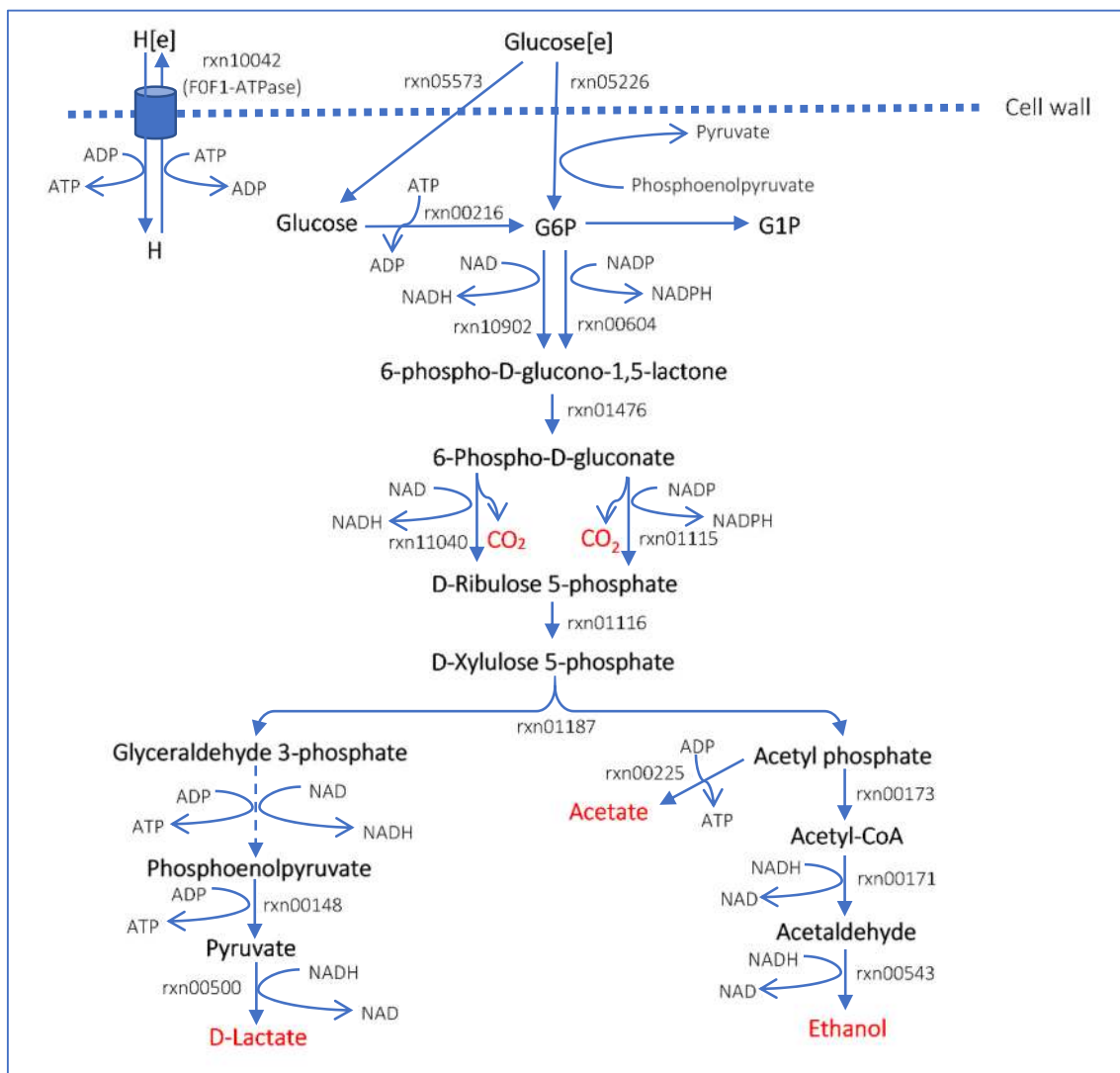
Fig. 1 Phosphoketolase pathway in the metabolic network of *L. mesenteroides* subsp. *cremoris*. Glucose is metabolized through PKP where one glucose 6-phosphate is broken down into two branches resulting in equal molar of glyceraldehyde 3-phosphate and acetyl phosphate. When glucose is the sole carbon source, the branch where glyceraldehyde 3-phosphate is converted into lactate is redox balanced and produces ATP required for the cell, while on the other branch, acetyl phosphate is converted into ethanol resulting in NADH oxidation or into acetate by acetate kinase resulting in ATP. The conversion of acetyl phosphate into acetate or ethanol is governed by the redox balance and ATP requirement of the cell. Metabolites represented by red color are major external metabolites produced. G6P, D-Glucose 6-phosphate; G1P, D-Glucose 1-phosphate. Reaction IDs given in the figure are the reaction IDs in the genome-scale model. Full reaction IDs are in Supporting Information-I

Understanding the metabolism of *L. mesenteroides* may help the efficient use of this important lactic acid bacterium in the industry. Although the classical studies investigating *L. mesenteroides* at external metabolite level give important insights into the metabolism, systems biology approaches (Nielsen 2017) are more promising to decipher the full metabolic potential of *L. mesenteroides* at genome scale. Recently, with the advent of the next generation sequencing technology, various studies investigating the genomic characterization of *L. mesenteroides* strains (Chun et al. 2017; Frantzen et al. 2017) have been published.

Genome-scale metabolic models (GSMMs) are very useful tools to investigate the metabolic patterns and capacities of organisms, and they have already been developed for quite a number of LAB, such as probiotic strains *Lactobacillus plantarum* (Teusink et al. 2006), *Lactobacillus casei* (Vinay-Lara et al. 2014); dairy-origin strains *Lactococcus lactis* subsp. *lactis* (Oliveira et al. 2005), *Lactococcus lactis* subsp. *cremoris* (Flahaut et al. 2013), *Streptococcus thermophilus* (Pastink et al. 2009), and a plant-origin *L. mesenteroides* subsp. *mesenteroides* (Koduru et al. 2017). GSMMs are used not only to investigate the metabolic pattern of an organism, but also to compare the metabolic capacities of different organisms. Comparison of the dairy-origin LAB using GSMMs is also important to better understand the fermentation of the dairy foods where different LAB take part in co-culture. *L. lactis*, *S. thermophilus*, and *L. mesenteroides* species are major LAB used in cheese starter cultures at different combinations, based on cheese type (Cogan et al. 2007; Leroy and De Vuyst 2004; Smid et al. 2014). Thus, a GSMM of dairy-origin *L. mesenteroides* was missing and needed to better understand its contribution to cheese fermentation.

In this study, for the first time, GSMM of a dairy-origin *Leuconostoc mesenteroides* subsp. *cremoris* ATCC 19254 was reconstructed, and model simulations were compared with experimental and literature-based data. Growth rate and product profiles strongly depended on the energetics and redox state of the organism, and the metabolic model explained in detail the metabolic mechanisms behind these patterns. Moreover, only few LAB such as dairy-origin *L. lactis* subsp. *lactis* biovar. *diacetylactis*, *L. mesenteroides* (Smid et al. 2014) and cocoa bean fermentation-origin *Lactobacillus fermentum*, *Lactobacillus plantarum* (Adler et al. 2013) are known to be citrate consumers, and citrate utilization in *L. mesenteroides* leads to stimulation in growth and increases flavor formation (Schmitt et al. 1992; Starrenburg and Hugenholtz 1991). Our genome-scale model has incorporated citrate utilization and citrate-related flavor metabolism, allowing to simulate citrate and glucose co-metabolism and flavor production potential in *L. mesenteroides*.

Materials and methods

Organism, fermentation conditions, and experimental analyses

Dairy-origin *L. mesenteroides* subsp. *cremoris* ATCC 19254 used in this study was purchased from American Type Culture Collection (ATCC). Chemically defined medium (CDM) described in literature (Otto et al. 1983) and modified elsewhere (Poolman and Konings 1988) was used for the preparation of the inoculum and for the fermentation culture, and the CDM was filter-sterilized with 0.22-μm filters. The organism was fermented at anaerobic conditions in a 5-l stirred tank bioreactor (Minifors HT, Switzerland) with a working volume of 3l. Fermentation medium was deoxygenized with pure N_2 supply before inoculation, and anaerobic condition was maintained by sterile N_2 supply with 0.5 vvm during fermentation. The bioreactor was inoculated with 2% (*v/v*) inoculum culture at the end of the exponential phase. Anaerobic fermentation was carried out at constant temperature (30 °C) with 100 rpm mixing rate and without pH control. Biomass concentration was determined using optical density (OD) measurements of fermentation culture at 600 nm, which was then correlated with corresponding biomass dry weight (gDW) via a calibration graph. Based on this, one unit of optical density at 600 nm was taken as equivalent to 0.37 g dry cell weight/l. Culture samples were centrifuged at 10,000×*g* for 10 min to separate biomass and supernatant, and cell-free supernatant was used for glucose, organic acid, and amino acid analyses. Glucose concentration was determined by reducing sugar analysis (Miller 1959). Organic acid (lactic, formic, acetic, and citric acids) concentrations were determined using HPLC with an anion exchange column (IC-Pak Ion exclusion column (7 μm, 7.8 × 300 mm, Waters)) and UV detector with 2 mM H_2SO_4 as mobile phase and with 0.5 ml/min flow rate. Amino acids were quantified using HPLC with pre-column derivatization using phenyl isothiocyanate (PITC), following a modified version of the method described in literature (Shi et al. 2013). HPLC (LC20AD, Shimadzu) was equipped with a UV detector (254 nm) and XSelect HSS C18 column (5 μm, 4.6 mm × 250 mm, Waters) maintained at 36 °C. Two mobile phases (0.1 M pH 6.5 sodium acetate buffer solution:acetonitrile (97:3(*v/v*)) and acetonitrile:water (4:1(*v/v*)) are used, at 0.9 ml/min molar reaction rates of ethanol and CO_2 were estimated based on the consumed glucose following the stoichiometry observed in heterolactic fermentation of *L. mesenteroides* in anaerobic conditions with glucose as the only carbon source (Dols et al. 1997; Schmitt et al. 1992; Starrenburg and Hugenholtz 1991), and this ratio was taken as rates of glucose:ethanol:CO_2 = 1:1:1. For citrate and glucose co-metabolism, production of 1 mol of CO_2 was considered per 1 mol citrate consumed.

Essential amino acid requirements for *L. mesenteroides* subsp. *cremoris* ATCC 19254 were experimentally determined by amino acid omission experiments. Centrifuged inoculum culture was washed twice and re-suspended with sterile pure water with 0.9 % NaCl. CDM broth with all amino acids (reference culture) and CDM broths with omitted individual amino acids were inoculated (2% *v/v*) using the amino acid-free inoculum culture. They were incubated at 30 °C for 48 h in static cultures. The OD of the cultures at 600 nm was then measured as an indication for growth. All experiments were repeated at least twice.

Genome annotation

L. mesenteroides subsp. *cremoris* ATCC 19254 was sequenced as part of the Human Microbiome Project (Human Microbiome Project 2012a; Human Microbiome Project 2012b). The complete genome sequence of *L. mesenteroides* subsp. *cremoris* ATCC 19254 (GenBank accession number GCA_000160595.1) is available online at National Center for Biotechnology Information (NCBI) (http://www.ncbi.nlm.nih.gov). The genome sequence was imported into the RAST server (http://rast.nmpdr.org/) for gene calling and annotation (the statistics for the genome and annotation of *L. mesenteroides* ATCC 19254 can be found in Supporting Information-I).

Reconstruction of *L. mesenteroides* subsp. *cremoris* metabolic network at genome scale

A genome-scale metabolic draft model for *L. mesenteroides* subsp. *cremoris* ATCC 19254 was generated using the ModelSEED database (Henry et al. 2010). The genome of *L. mesenteroides* ATCC 19254 was also uploaded to the following databases in order to recover the functions missing in the ModelSEED annotation: (i) MetaDraft (B.G. Olivier 2018. [Online], https://systemsbioinformatics.github.io/metadraft) which generates genome-scale metabolic draft models based on existing well-curated models, (ii) a KEGG-based database BlastKOALA (http://www.kegg.jp/blastkoala/) which gives genome annotations and related functions of the genome, and (iii) TransportDB 2.0 (www.membranetransport.org/) which lists membrane transport proteins. Experimental and literature-based studies were used for the manual curation of the draft model (see Supporting Information-I for the complete reaction list and related gene-reaction associations). The biomass composition of *L. mesenteroides* used for the biomass reaction in the reconstructed model was obtained from the literature. Protein, lipid, DNA, RNA, and polysaccharide contents as major biopolymers and compositions of building blocks such as amino acids, nucleotides, and fatty acids forming these biopolymers are based on species or strain specific data (Bang et al. 2017; Harney et al. 1967; Tracey and

Britz 1989), while other minor compositions are based on the data of phylogenetically close LAB (Flahaut et al. 2013; Oliveira et al. 2005; Pastink et al. 2009; Teusink et al. 2006; Vinay-Lara et al. 2014) (see the Supporting Information-II for the details). The values of growth associated maintenance (GAM, K_x) and non-growth associated maintenance (NGAM, m_{ATP}) were calculated via Pirt Equation ($\sum q_{ATP,\ i} - K_X\mu - m_{ATP} = 0$) using the experimental data (Dols et al. 1997) that estimates the rates of energy synthesis (q_{ATP}) with respect to growth rates (μ) for various sugar sources for *L. mesenteroides* in batch cultures (see Supporting Information-II). Consequently, 30.651 mmol/gDW and 0.51 mmol/gDW/h were used as GAM and NGAM values for this study.

Metabolic flux distributions were estimated via flux balance analysis (FBA) (Orth et al. 2010) and flux variability analysis (FVA) (Mahadevan and Schilling 2003). Biomass production was maximized as the objective function in FBA to obtain the metabolic flux distributions by constraining the carbon source and amino acid uptake rates to fixed and maximal values, respectively. The constraints used in the analyses are listed in Supporting Information-I. Manual curation of the draft model and all constraint-based metabolic flux analyses were performed using COBRA Toolbox (Schellenberger et al. 2011) in MATLAB environment with Gurobi6 (http://www.gurobi.com) as the optimization solver.

Results

Model reconstruction and validation

The draft metabolic model initially reconstructed by the automatic reconstruction tools (see "Materials and methods") was subsequently manually curated using our experimental data and literature-based results. After adding the species-specific biomass reaction, amino acid requirements were predicted by the draft model using FBA, through maximizing the growth rate while consecutively constraining the individual amino acid uptake rates to zero. Amino acid requirements predicted by the draft model were then compared with the experimental results, and inconsistencies between in silico and in vitro results were used to manually curate the draft model (Table 1).

Although there was no growth without alanine, asparagine, phenylalanine, and tyrosine in silico, *L. mesenteroides* grew without these amino acids in vitro. This indicated that biosynthesis pathways of these amino acids were not complete or not available in the genome annotation of *L. mesenteroide*s ATCC 19254. Therefore, the required reactions for the biosynthesis of alanine, asparagine, phenylalanine, and tyrosine were added to the draft model based on the biosynthesis

Table 1 Essential amino acids obtained via in vitro and in silico analyses. *R*, required for growth; *NR*, not required for growth

	Experimental results* (OD at 600 nm)	Draft model	Curated model
Control	1.310	NR	NR
Alanine	1.187	R	NR
Arginine	0.060	NR	NR
Aspartate	1.204	NR	NR
Asparagine	1.258	R	NR
Cysteine	0.158	R	R
Glutamate	1.237	NR	NR
Glutamine	1.239	NR	NR
Glycine	1.253	NR	NR
Histidine	0.203	NR	NR
Isoleucine	0.089	NR	NR
Leucine	0.124	NR	NR
Lysine	0.068	R	R
Methionine	0.163	R	R
Phenylalanine	1.136	R	NR
Proline	1.266	NR	NR
Serine	1.251	NR	NR
Threonine	0.829	NR	NR
Tryptophan	0.082	NR	NR
Tyrosine	1.228	R	NR
Valine	0.093	NR	NR
Prediction ratio by models		12/20	16/20

*Data shown are the averages of three repetitive cultures

Maximal optical densities observed were classified as amino acid required for growth (OD < 0.20) and amino acid not required for growth (OD > 0.20).

mechanisms observed on previous LAB metabolic models (Flahaut et al. 2013; Oliveira et al. 2005; Pastink et al. 2009; Teusink et al. 2006). See Supporting Information-I for the reactions added.

Arginine, tryptophan, and the branched-chain amino acids (leucine, isoleucine, and valine) were not essential according to the computational analysis with the draft model; however, they were identified as essential amino acids based on our experimental results. This unexpected result may be explained by the feedback inhibition of the synthesis of some amino acids in the presence of other amino acids, which was also reported in literature (Teusink et al. 2005). In that study, for example, although the complete pathway for tryptophan synthesis existed in genome annotation, no growth was observed when tryptophan was omitted from the medium, and a reasonable growth was observed when other aromatic amino acids (tyrosine or phenylalanine) were also omitted (Teusink et al. 2005). In silico growth was observed with not only individual omission of the branched-chain amino acids (leucine, isoleucine, and valine), but also simultaneous omission of these three amino acids. On the other hand, there was no in silico growth with omission of glutamine and glutamate together,

which shows that glutamate and glutamine are not synthesized individually but compensate each other if needed.

Glucose 6-phosphate dehydrogenase (G6PDH) of *L. mesenteroides* can utilize either NAD or NADP, and this unusual dual coenzyme specificity of the G6PDH from *L. mesenteroides* was reported by several studies (Cosgrove et al. 1998; Levy 1989; Levy et al. 1983; Naylor et al. 2001; Olive et al. 1971). Only NADP-specific G6PDH existed in the draft metabolic model, and it caused excessive production of NADPH, which was re-oxidized by biologically irrelevant ways in the network. Thus, NAD-specific G6PDH reaction was added to the draft model. In the final model, NADH generated by the NAD-specific G6PDH and NADPH generated by the NADP-specific G6PDH were re-oxidized in the reductive steps of heterolactic fermentation and biosynthesis of lipid, respectively.

Upon manual curation, the final metabolic model contained 1129 metabolites and 1088 reactions governed by 559 genes and is named as *iLM.c559*. The reconstructed model is available in SBML format in Supporting Information-III.

After manual curation, the model was compared with our anaerobic experimental data for validation (Table 2).

Table 2 Experimental and computational reaction rates of the co-metabolism of citrate and glucose for anaerobic fermentation of *L. mesenteroides* subsp. *cremoris*. The objective function (growth rate) flux value was obtained by FBA, and minimum and maximum in silico flux values of production rates were obtained by FVA. Reaction rates for the experimental values were calculated for the exponential phase of batch fermentation (2–14 h). Uptake rates of amino acids obtained by experimental analysis were constrained as maximum uptake rates of amino acids in the model. Note that the measured reaction rates indirectly reflect the effect of changing pH in the fermentation. See the Supporting Information-I for the amino acid uptake rates used

Reaction	In vitro reaction rates	In silico reaction rates
Glucose uptake rate	5.03	5.03 [1]
Citrate uptake rate	1.17	1.17 [1]
Lactate production rate	5.29	4.80–5.80
Ethanol production rate	5.03 [2]	3.85–4.43
Acetate production rate	1.53	1.38–1.76
CO_2 production rate	6.20 [2]	5.88–6.94
Flavor metabolite [3] production rate	NM	0–0.77
Growth rate (1/h)	0.15	0.14

NM not measured

[1] Constrained value

[2] Ethanol and CO_2 were not measured experimentally, but they were calculated based on experimental consumption rates (see Experimental Procedures)

[3] Flavor metabolites: the summed production rates of acetyl, diacetyl, 2,3-Butandiol, 4-Methyl-2-oxopentanoate (4MOP), (S)-3-Methyl-2-oxopentanoate (3MOP), and 3-Methyl-2-oxobutanoate (3MOB)

Experimental results showed a typical heterolactic fermentation pattern; half of the carbon sources consumed were converted to lactate, and the rest of the carbon sources were converted to ethanol, acetate, and CO_2 (see Supporting Information-I for the batch fermentation data). The consistency between experimental and computational growth rates provided a validation of the reconstructed genome-scale metabolic model, iLM.c559. It also showed that the calculated values of the energetic parameters (GAM and NGAM) used in the model were acceptable for *L. mesenteroides*.

Model-based investigation of heterolactic fermentation and flavor metabolism in *L. mesenteroides* subsp. *cremoris* in anaerobic conditions

The reconstructed metabolic model showed that heterolactic fermentation of *L. mesenteroides* is governed by energy and redox balances, as stated by several studies (Koduru et al. 2017; Plihon et al. 1995; Schmitt et al. 1992). At first, the reconstructed model was used to simulate heterolactic fermentation behavior of the organism, detailed in Fig. 1, under glucose-only anaerobic conditions. Product formation rates were calculated as a function of increase in the glucose consumption rates (Fig. 2a). The model predicted that glucose—as the only carbon source—was converted to lactate, ethanol, and CO_2 with almost equal glucose:product molar ratio of glucose:CO_2:lactate:ethanol:acetate = 1:1:1:1:0 (Fig. 2a). This ratio was also observed by several experimental studies for the anaerobic fermentation of *L. mesenteroides* (Bourel et al. 2003; LevataJovanovic and Sandine 1996; Plihon et al. 1995).

When citrate was used as the sole carbon source, in silico growth was not observed, which is also consistent with an experimental study (Starrenburg and Hugenholtz 1991). The metabolic model was then simulated by changing citrate rates at a fixed glucose consumption rate (Fig. 2b). Because citrate acts as an electron acceptor, in silico growth was stimulated by the co-utilization of citrate, again in agreement with the experimental studies associated with the citrate consumption of *L. mesenteroides* (Schmitt et al. 1992; Starrenburg and Hugenholtz 1991). In flux predictions, citrate contributes to the pyruvate pool through oxaloacetate decarboxylase (Fig. 3), which is also stated in literature (LevataJovanovic and Sandine 1996). The pyruvate derived from citrate utilization increased the lactate production, which led to an increase in the oxidation of NADH. Therefore, the cell needed to make less ethanol for the oxidation of NADH, and hence some part of acetyl phosphate could be converted to acetate by acetate kinase resulting in additional ATP production. Stimulation of growth could be explained by the increase in available ATP through acetate production. The increased lactate production with increased citrate, as well as the decreased ethanol formation, in our model prediction is consistent with the studies of Schmitt et al. (1992) and Schmitt and Divies (1992) respectively. In addition to indirect contribution of citrate to acetate production by acetate kinase (rxn00225 in Fig. 1), citrate also directly contributes to the acetate pool by citrate oxaloacetate-lyase (rxn00265 in Fig. 3).

Fig. 2 Effect of glucose and citrate uptake rates on metabolite production profile and growth rate, obtained by model simulations. Width of the flux profiles denotes flux span obtained by FVA. **a** Product profiles with respect to glucose consumption rate when glucose is the sole carbon source. **b** Product profiles with co-metabolism of citrate and glucose. Glucose is fixed to a constant consumption rate (15 mmol/gDW/h) for this analysis. Maximum uptake rates of amino acids were constrained to 0.2 mmol/gDW/h for **a** and **b**. Flavor: the summed rates of acetyl, diacetyl, 2,3-Butandiol, 4-Methyl-2-oxopentanoate (4MOP), (S)-3-Methyl-2-oxopentanoate (3MOP), and 3-Methyl-2-oxobutanoate (3MOB)
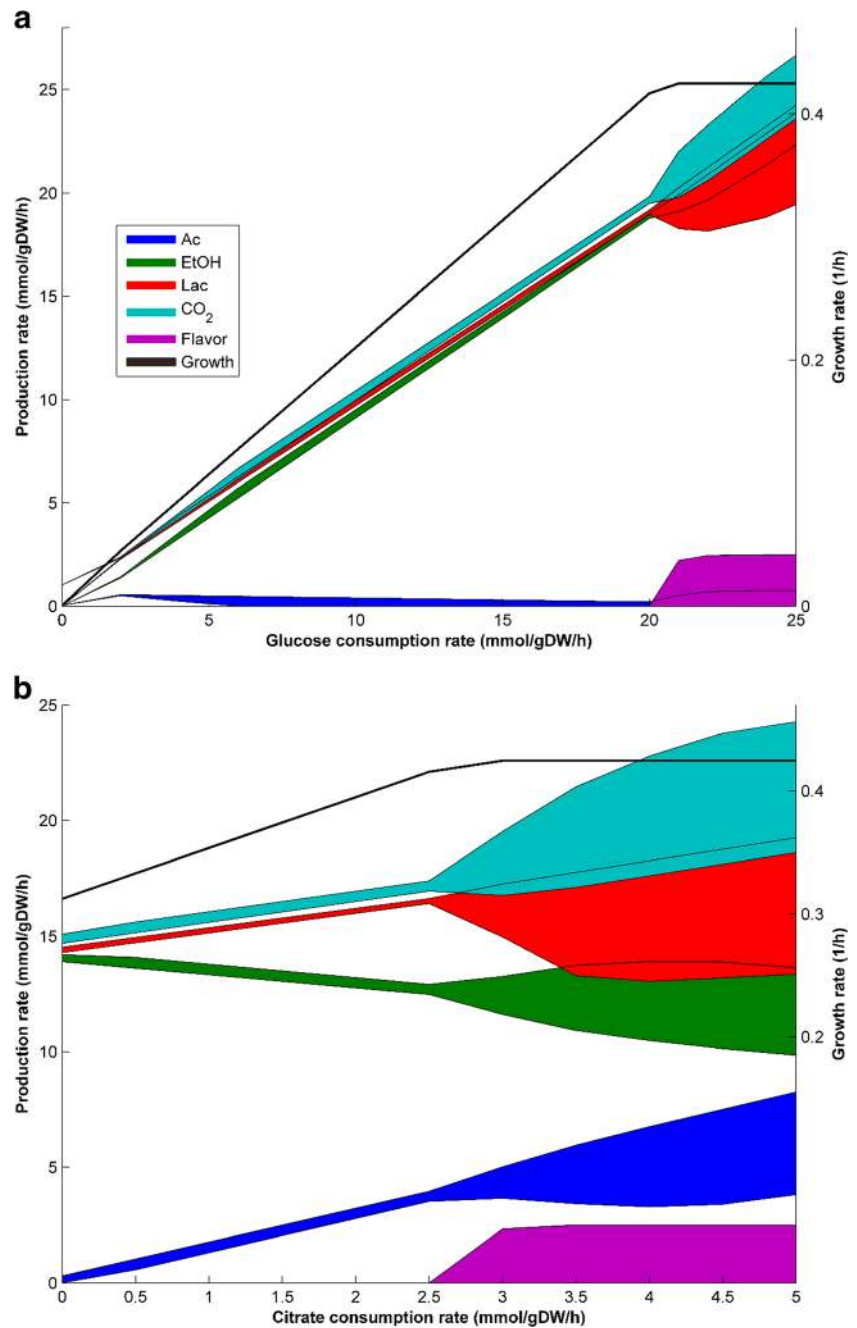
Citrate utilization leads to the production of flavor metabolites in *L. mesenteroides* (LevataJovanovic and Sandine [1996](#); Schmitt et al. [1992](#); Starrenburg and Hugenholtz [1991](#)). In our model, flavor metabolites produced following the routes seen in Fig. 3 are acetoin, diacetyl, 2,3-butanediol, 4-methyl-2-oxopentanoate (4MOP), (S)-3-methyl-2-oxopentanoate (3MOP), and 3-methyl-2-oxobutanoate (3MOB), the last three of which are associated with amino acid metabolism. Flavor metabolite production was observed not only with co-metabolism of citrate and glucose (Fig. 2b), but also with glucose as the only carbon source (Fig. 2b).

However, significant production was only observed when the growth rate could not increase anymore due to amino acid limitation. Because of excess carbon and ATP, the flux span of products obtained by FVA widens after this point. Whereas minimum flux values of lactate and acetate production decreased, maximum flux values of flavor metabolites production increased. This result shows that the cell can divert the carbon sources to flavor production when it has no growth requirements (carbon or ATP) anymore. The amount of molar carbon required to reach the maximal growth rate, and hence flavor formation, was lower when

Fig. 3 Flavor metabolite production associated with citrate metabolism. Metabolites represented by red color are external metabolites produced. 4MOP, 4-Methyl-2-oxopentanoate; 3MOP, (S)-3-Methyl-2-oxopentanoate; 3MOB, 3-Methyl-2-oxobutanoate

glucose and citrate were co-metabolized compared to sole glucose consumption (Fig. 2). This may indicate how citrate can be advantageous for flavor production.

In line with our model predictions, the production of aromatic compounds was favored over the synthesis of other metabolites from citrate during the stationary phase (LevataJovanovic and Sandine 1996). Moreover, a recent study about the aroma formation from a citrate-consuming dairy *Lactococcus lactis* at near-zero growth rates points out that some particular LAB can survive in long periods of nutrient limitation, as in the case of cheese ripening, and these LAB still contribute to the flavor formation (van Mastrigt et al. 2018). We therefore investigated the flavor metabolite production during co-metabolism of citrate and glucose at low growth rates in silico: growth rate was fixed to near-zero values, and flux distributions were calculated constraining carbon and nitrogen sources to low values to mimic nutrient limitation conditions, with the maximization of ATP production as the

objective function. As expected, production of total flavor metabolites linearly increased, and acetate and lactate production decreased with decreasing growth rate (data not shown).

Metabolic shift and stimulation of growth in *L. mesenteroides* subsp. *cremoris* under aerobic conditions

Although acetate production by acetate kinase supplies ATP for the cell, significant amount of acetyl phosphate is converted into ethanol to balance the redox state of the cell by producing NAD under anaerobic conditions. The bottleneck of obligate heterolactic *L. mesenteroides* due to energy and redox state could be overcome by aerobic fermentation. The reconstructed metabolic model was used to simulate aerobic conditions. Simulation results showed that oxygen acted as another electron acceptor for *L. mesenteroides*, and NADH was oxidized by aerobic fermentation, which is also observed in the respiration of some LAB (Pedersen et al. 2012). The membrane-associated mechanisms of *L. mesenteroides* suggested by the metabolic model for aerobic conditions are illustrated in Fig. 4. Then, the protons extruded by the respiratory mechanism could be utilized by the F0F1-ATPase to generate ATP. Thus, under aerobic conditions, the requirement of ethanol production for re-oxidation of NADH decreases and acetate production increases. This phenomenon causes a metabolic shift between ethanol and acetate production and stimulates the cell growth (Fig. 5) due to ATP production by acetate kinase and F0F1-ATPase. Hence, the stoichiometric ratio of glucose:ethanol:acetate could be summarized as 1:1:0 and 1:0:1 for anaerobic and fully aerobic fermentation of *L. mesenteroides* respectively, which is also reported by several experimental studies associated with *L. mesenteroides* (Bourel et al. 2003; Dols et al. 1997; Plihon et al. 1995). The same simulation also showed that increasing oxygen uptake rates had minimal effect on lactate and CO_2 production rates (Fig. 5), in agreement with an experimental study (Plihon et al. 1995).

The model also predicted flavor production with increasing oxygen uptake rate (Fig. 5), but similar to the simulations in anaerobic conditions, significant amount of flavor metabolites production was observed only after the oxygen-induced

Fig. 4 Respiration mechanisms mediated by menaquinone-8 and ubiquinone-8 in *L. mesenteroides* subsp. *cremoris*. NADH is not oxidized by oxygen directly, but rather NADH is oxidized by menaquinone or ubiquinone, which is re-oxidized by oxygen.

Fig. 5 Model predictions on the metabolic shift between ethanol and acetate production by increasing oxygen uptake rate. Glucose uptake rate as only carbon source was fixed to 10 mmol/gDW/h, and maximum uptake rates of amino acids were fixed to 0.2 mmol/gDW/h. Growth, circle; CO_2, square; lactate, cross sign; acetate, triangle; ethanol, inverted triangle; flavor, star

growth increase saturated. Flux span patterns obtained by FVA (see Supporting Information-I) was also similar to the co-metabolism of glucose and citrate in anaerobic condition, which was discussed above.

Effect of different carbon sources on growth profiles in *L. mesenteroides* subsp. *cremoris*

In addition to aerobic fermentation, another strategy to overcome the energy and redox state bottleneck in *L. mesenteroides* could be the use of different carbon sources. For this purpose, growth and product profiles were simulated by the model for commonly used mono and disaccharides as

carbon sources, the utilization mechanisms of which were illustrated in Fig.6.

Consumption rates of monosaccharides (glucose and fructose) were fixed to twice the disaccharides (sucrose and lactose) consumption rates to simulate the equivalent carbon utilization rates. Another constraint was applied for the ethanol production in fructose growth by fixing its rate to zero according to the experimental study (Dols et al. 1997) because it was necessary for the simulation of non-zero mannitol production by fructose utilization. The model predicted the oxidation of NADH by mannitol production since the oxidation route via ethanol production was inactive in the fructose fermentation. The usage of significant amounts of the fructose for mannitol

Fig. 6 Representation of the utilization of commonly used carbon sources by *L. mesenteroides* subsp. *cremoris*. G6P, Glucose 6-phosphate; G1P, Glucose 1-phosphate; F6P, Fructose 6-phosphate; GAL1P, Galactose 1-phosphate
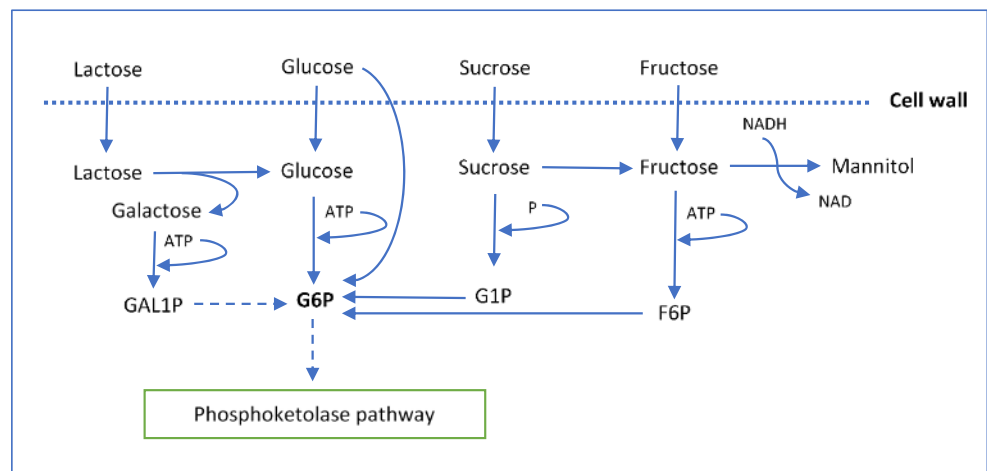
production led to the decrease in growth rate compared to other carbon sources. On the other hand, the growth was stimulated with the utilization of sucrose as a carbon source (Fig. 7) because less ATP was consumed per equivalent carbon utilization rate compared to the other carbon sources (Fig. 6). A decrease and increase of growth on fructose and sucrose, respectively, is consistent with literature (Dols et al. 1997). Although the consumed ATP per equivalent carbon utilization rate was the same for glucose and lactose, in silico growth rate decreased with lactose utilization due to the difference in transport systems of these two sugar sources. Lactose is transferred by proton symport, which is the only transport mechanism for lactose in the model, whereas glucose is transferred by a phosphotransferase system (PTS), which is energetically more advantageous. Our model explains the reason behind this advantage. F0F1-ATPase is a membrane-bound enzyme that pumps out the intracellular proton using ATP in anaerobic conditions in LAB for pH homeostasis (Konings 2002), and F0F1-ATPase in our model also has the same task for anaerobic conditions. Contrary to the proton symport used as a lactose transport system, the PTS, used as a glucose transport system in the model, does not introduce intracellular proton. Hence, F0F1-ATPase spent less ATP to pump protons out.

Discussion

In this work, the first GSMM of dairy-origin *L. mesenteroides* subsp. *cremoris* ATCC 19254 was reconstructed and analyzed. The model is the second *L. mesenteroides* reconstruction in the

literature after the plant-origin *L. mesenteroides* subsp. *mesenteroides* ATCC 8293 (Koduru et al. 2017). In terms of their genome sizes, the two subspecies are the most distinct ones among 17 subspecies (Chun et al. 2017). The plant-origin subspecies has the biggest genome size among 17 subspecies (2.08 Mb) whereas the cheese-origin subspecies has the lowest genome size (1.74 Mb). The difference is also reflected in the number of genes. The subspecies reconstructed and analyzed in this work has around 300 genes less than the plant-origin subspecies. Genome comparison of dairy-origin *L. mesenteroides* ATCC 19254 and plant-origin *L. mesenteroides* ATCC 8293 show significant differences in the metabolism of the two, which include sucrose and amino acid metabolism in particular (See Supporting Information-I for the comparison of sucrose metabolism).

Our individual amino acid omission experiments showed that the absence of histidine causes weak growth and eight amino acids (arginine, cysteine, isoleucine, leucine, lysine, methionine, tryptophan, and valine) are required for the growth of the dairy-origin strain *L. mesenteroides*. However, only two amino acids (glutamine and valine) are essential for a plant-origin *L. mesenteroides* (Koduru et al. 2017). The amino acid auxotrophy differences between dairy and plant-origin *L. mesenteroides* supports the hypothesis in a study which, by stating the difference in amino acid auxotrophies for the dairy and plant-origin lactic acid bacterium *Lactococcus lactis*, proposes that dairy strains originate from the plant niche (Bachmann et al. 2012).

Fig. 7 Effect of commonly used carbon sources on the metabolic products of *L. mesenteroides* in anaerobic condition predicted by the model. Uptake rates of monosaccharides (glucose and fructose) and disaccharides (lactose and sucrose) were constrained to 10 and 5 mmol/gDW/h respectively (without citrate uptake), and maximum uptake rates of amino acids were constrained to 0.2 mmol/gDW/h. Ethanol production via fructose fermentation was fixed to zero (Dols et al. 1997). Error bars denote flux span obtained by FVA
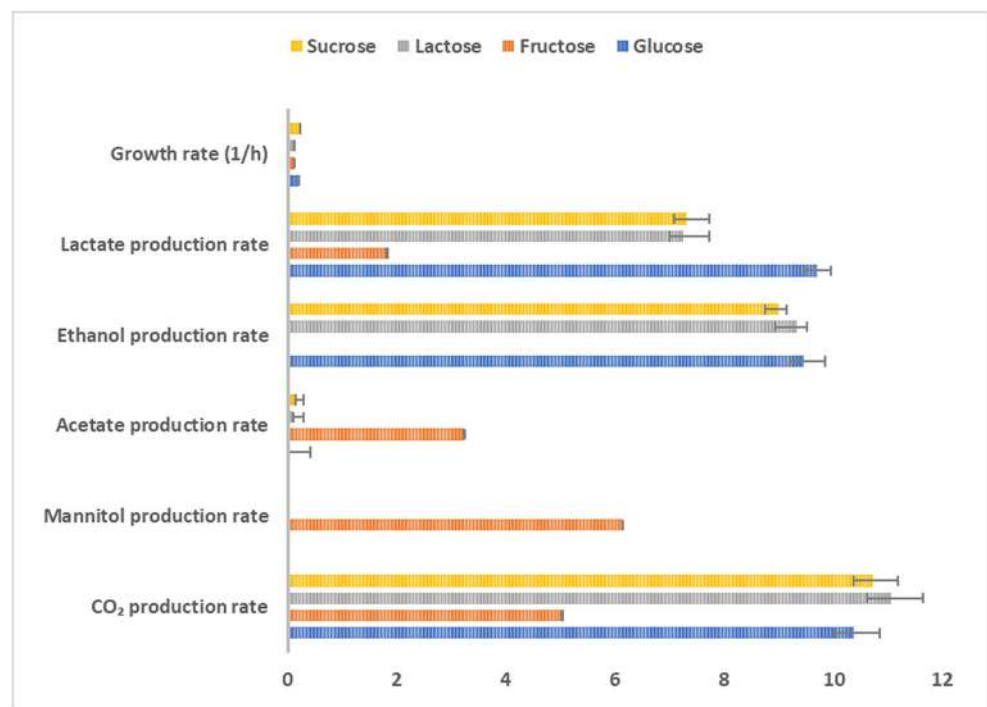
Upon simulation of our model, we realized an important difference in the redox state of the two models: In the plant-derived model, G6PDH and phosphogluconate dehydrogenase (GND) reactions of PKP produce only NADPH, which is re-oxidized via futile cycles not related with PKP, and NADH oxidized in ethanol production is also produced by futile cycles not related with PKP. But in our model, both G6PDH and GND have dual coenzyme specificity, and NADH and NADPH produced in PKP were re-oxidized in the reductive steps of heterolactic fermentation and biosynthesis of lipid, respectively. Finally, the metabolic model reconstructed in this study additionally incorporated the citrate utilization and citrate-related flavor metabolism, which was not considered in the plant-origin *L. mesenteroides* model. This allowed us to investigate the role of citrate metabolism and oxygen uptake on flavor formation.

There are several hypotheses about why microorganisms used in food fermentation processes produce flavor compounds (Carroll et al. 2016; Christiaens et al. 2014), and some mechanisms for flavor metabolite production could be inferred by our metabolic model. We found that flavor formation occurred only when increased carbon or oxygen uptake did not enhance growth rate anymore. In both cases, up until that point, oxygen and citrate created a redox sink that increased acetate formation, which increased ATP formation and growth rate. This suggests that flavor formation occurs under excess carbon and ATP. We also expect this effect when growth is inhibited by acidification while there is still carbon present. For citrate, this could mean two things: first, flavor formation from the imported citrate requires the absence of ATP demand by growth. Second, citrate uptake and metabolism occur irrespective of ATP demand by growth, and this "unneeded" citrate is excreted as waste products in the form of flavor compounds. This is a novel biological insight from the model that may be explored to enhance flavor formation in this aroma bacterium.

Compliance with ethical standards

Conflict of interest The authors declare that they have no conflict of interest.

Ethical approval This article does not contain any studies with human participants or animals performed by any of the authors.

References

Adler P, Bolten CJ, Dohnt K, Hansen CE, Wittmann C (2013) Core fluxome and metafluxome of lactic acid bacteria under simulated cocoa pulp fermentation conditions. Appl Environ Microbiol 79(18):5670–5681. https://doi.org/10.1128/AEM.01483-13

Bachmann H, Starrenburg MJ, Molenaar D, Kleerebezem M, van Hylckama Vlieg JE (2012) Microbial domestication signatures of *Lactococcus lactis* can be reproduced by experimental evolution. Genome Res 22(1):115–124. https://doi.org/10.1101/gr.121285.111

Bang J, Li L, Seong H, Kwon YW, Lee DY, Han NS (2017) Macromolecular and elemental composition analyses of *Leuconostoc mesenteroides* ATCC 8293 cultured in a chemostat. J Microbiol Biotechnol 27(5):939–942. https://doi.org/10.4014/jmb.1612.12038

Bourel G, Henini S, Divies C, Garmyn D (2003) The response of *Leuconostoc mesenteroides* to low external oxidoreduction potential generated by hydrogen gas. J Appl Microbiol 94(2):280–288

Campedelli I, Flórez AB, Salvetti E, Delgado S, Orrù L, Cattivelli L, Alegría Á, Felis GE, Torriani S, Mayo B (2015) Draft genome sequence of three antibiotic-resistant *Leuconostoc mesenteroides* strains of dairy origin. Genome Announc 3(5):e01018–e01015

Carroll AL, Desai SH, Atsumi S (2016) Microbial production of scent and flavor compounds. Curr Opin Biotechnol 37:8–15. https://doi.org/10.1016/j.copbio.2015.09.003

Christiaens JF, Franco LM, Cools TL, De Meester L, Michiels J, Wenseleers T, Hassan BA, Yaksi E, Verstrepen KJ (2014) The fungal aroma gene ATF1 promotes dispersal of yeast cells through insect vectors. Cell Rep 9(2):425–432. https://doi.org/10.1016/j.celrep.2014.09.009

Chun BH, Kim KH, Jeon HH, Lee SH, Jeon CO (2017) Pan-genomic and transcriptomic analyses of *Leuconostoc mesenteroides* provide insights into its genomic and metabolic features and roles in kimchi fermentation. Sci Rep 7(1):11504. https://doi.org/10.1038/s41598-017-12,016-z

Cogan TM, Beresford TP, Steele J, Broadbent J, Shah NP, Ustunol Z (2007) Invited review: advances in starter cultures and cultured foods. J Dairy Sci 90(9):4005–4021. https://doi.org/10.3168/jds.2006-765

Cosgrove MS, Naylor C, Paludan S, Adams MJ, Levy HR (1998) On the mechanism of the reaction catalyzed by glucose 6-phosphate dehydrogenase. Biochemistry 37(9):2759–2767. https://doi.org/10.1021/bi972069y

de Paula AT, Jeronymo-Ceneviva AB, Todorov SD, Penna ALB (2015) The two faces of *Leuconostoc mesenteroides* in food systems. Food Rev Int 31(2):147–171. https://doi.org/10.1080/87559129.2014.981825

Dols M, Chraibi W, Remaud-Simeon M, Lindley ND, Monsan PF (1997) Growth and energetics of *Leuconostoc mesenteroides* NRRL B-1299 during metabolism of various sugars and their consequences for dextransucrase production. Appl Environ Microbiol 63(6):2159–2165

Flahaut NAL, Wiersma A, van de Bunt B, Martens DE, Schaap PJ, Sijtsma L, dos Santos VAM, de Vos WM (2013) Genome-scale metabolic model for *Lactococcus lactis* MG1363 and its application to the analysis of flavor formation. Appl Microbiol Biotechnol 97(19):8729–8739. https://doi.org/10.1007/s00253-013-5140-2

Frantzen CA, Kot W, Pedersen TB, Ardo YM, Broadbent JR, Neve H, Hansen LH, Dal Bello F, Ostlie HM, Kleppen HP, Vogensen FK, Holo H (2017) Genomic characterization of dairy associated *Leuconostoc* species and diversity of *Leuconostocs* in undefined mixed mesophilic starter cultures. Front Microbiol 8:132. https://doi.org/10.3389/fmicb.2017.00132

Ganzle MG (2015) Lactic metabolism revisited: metabolism of lactic acid bacteria in food fermentations and food spoilage. Curr Opin Food Sci 2:106–117. https://doi.org/10.1016/j.cofs.2015.03.001

Garvie EI (1986) Genus *Leuconostoc*. In: Sneath PHA, Mair NS, Sharpe ME, Holt JG (eds) Bergey's manual of systematic bacteriology, 2nd edn. Springer-Verlag, New York

Gaspar P, Carvalho AL, Vinga S, Santos H, Neves AR (2013) From physiology to systems metabolic engineering for the production of biochemicals by lactic acid bacteria. Biotechnol Adv 31(6):764–788. https://doi.org/10.1016/j.biotechadv.2013.03.011

Gunsalus IC, Gibbs M (1952) The heterolactic fermentation. II. Position of C14 in the products of glucose dissimilation by *Leuconostoc mesenteroides*. J Biol Chem 194(2):871–875

Guzel-Seydim ZB, Kok-Tas T, Greene AK, Seydim AC (2011) Review: functional properties of kefir. Crit Rev Food Sci Nutr 51(3):261–268. https://doi.org/10.1080/10408390903579029

Harney SJ, Simopoulos ND, Ikawa M (1967) Cell wall constituents of *Leuconostoc citrovorum* and *Leuconostoc mesenteroides*. J Bacteriol 93(1):273–277

Hemme D, Foucaud-Scheunemann C (2004) *Leuconostoc*, characteristics, use in dairy technology and prospects in functional foods. Int Dairy J 14(6):467–494. https://doi.org/10.1016/j.idairyj.2003.10.005

Henry CS, DeJongh M, Best AA, Frybarger PM, Linsay B, Stevens RL (2010) High-throughput generation, optimization and analysis of genome-scale metabolic models. Nat Biotechnol 28(9):977–982. https://doi.org/10.1038/nbt.1672

Human Microbiome Project C (2012a) A framework for human microbiome research. Nature 486(7402):215–221. https://doi.org/10.1038/nature11209

Human Microbiome Project C (2012b) Structure, function and diversity of the healthy human microbiome. Nature 486(7402):207–214. https://doi.org/10.1038/nature11234

Koduru L, Kim Y, Bang J, Lakshmanan M, Han NS, Lee DY (2017) Genome-scale modeling and transcriptome analysis of *Leuconostoc mesenteroides* unravel the redox governed metabolic states in obligate heterofermentative lactic acid bacteria. Sci Rep 7(1):15721. https://doi.org/10.1038/s41598-017-16026-9

Konings WN (2002) The cell membrane and the struggle for life of lactic acid bacteria. Antonie Van Leeuwenhoek 82(1-4):3–27

Leroy F, De Vuyst L (2004) Lactic acid bacteria as functional starter cultures for the food fermentation industry. Trends Food Sci Technol 15(2):67–78. https://doi.org/10.1016/j.tifs.2003.09.004

LevataJovanovic M, Sandine WE (1996) Citrate utilization and diacetyl production by various strains of *Leuconostoc mesenteroides* ssp *cremoris*. J Dairy Sci 79(11):1928–1935. https://doi.org/10.3168/jds.S0022-0302(96)76562-1

Levy HR (1989) Glucose-6-phosphate dehydrogenase from *Leuconostoc mesenteroides*. Biochem Soc Trans 17(2):313–315

Levy HR, Christoff M, Ingulli J, Ho EM (1983) Glucose-6-phosphate dehydrogenase from *Leuconostoc mesenteroides*: revised kinetic mechanism and kinetics of ATP inhibition. Arch Biochem Biophys 222(2):473–488

Mahadevan R, Schilling CH (2003) The effects of alternate optimal solutions in constraint-based genome-scale metabolic models. Metab Eng 5(4):264–276

Miller GL (1959) Use of Dinitrosalicylic Acid Reagent for Determination of Reducing Sugar. Anal Chem 31(3):426–428. https://doi.org/10.1021/ac60147a030

Naylor CE, Gover S, Basak AK, Cosgrove MS, Levy HR, Adams MJ (2001) NADP+ and NAD+ binding to the dual coenzyme specific enzyme *Leuconostoc mesenteroides* glucose 6-phosphate dehydrogenase: different interdomain hinge angles are seen in different binary and ternary complexes. Acta Crystallogr D Biol Crystallogr 57(Pt 5):635–648

Nielsen J (2017) Systems biology of metabolism. Annu Rev Biochem 86:245–275. https://doi.org/10.1146/annurev-biochem-061516-044757

Olive C, Geroch ME, Levy HR (1971) Glucose 6-phosphate dehydrogenase from *Leuconostoc mesenteroides*. Kinetic studies. J Biol Chem 246(7):2047–2057

Oliveira AP, Nielsen J, Forster J (2005) Modeling *Lactococcus lactis* using a genome-scale flux model. Bmc Microbiol 5:39. https://doi.org/10.1186/1471-2180-5-39

Orth JD, Thiele I, Palsson BO (2010) What is flux balance analysis? Nat Biotechnol 28(3):245–248. https://doi.org/10.1038/nbt.1614

Otto R, Tenbrink B, Veldkamp H, Konings WN (1983) The relation between growth-rate and electrochemical proton gradient of *Streptococcus cremoris*. FEMS Microbiol Lett 16(1):69–74

Pastink MI, Teusink B, Hols P, Visser S, de Vos WM, Hugenholtz J (2009) Genome-scale model of *Streptococcus thermophilus* LMG18311 for metabolic comparison of lactic acid bacteria. Appl Environ Microbiol 75(11):3627–3633. https://doi.org/10.1128/AEM.00138-09

Pedersen MB, Gaudu P, Lechardeur D, Petit MA, Gruss A (2012) Aerobic respiration metabolism in lactic acid bacteria and uses in biotechnology. Annu Rev Food Sci Technol 3:37–58. https://doi.org/10.1146/annurev-food-022811-101,255

Plihon F, Taillandier P, Strehaiano P (1995) Oxygen effect on batch cultures of *Leuconostoc mesenteroides* - relationship between oxygen-uptake, growth and end-products. Appl Microbiol Biotechnol 43(1):117–122

Poolman B, Konings WN (1988) Relation of growth of *Streptococcus lactis* and *Streptococcus cremoris* to amino-acid transport. J Bacteriol 170(2):700–707

Schellenberger J, Que R, Fleming RM, Thiele I, Orth JD, Feist AM, Zielinski DC, Bordbar A, Lewis NE, Rahmanian S, Kang J, Hyduke DR, Palsson BO (2011) Quantitative prediction of cellular metabolism with constraint-based models: the COBRA Toolbox v2.0. Nat Protoc 6(9):1290–1307. https://doi.org/10.1038/nprot.2011.308

Schmitt P, Divies C (1992) Effect of varying citrate levels on C-4 compound formation and on enzyme levels in *Leuconostoc mesenteroides* subsp *cremoris* grown in continuous culture. Appl Microbiol Biotechnol 37(4):426–430

Schmitt P, Divies C, Cardona R (1992) Origin of end-products from the co-metabolism of glucose and citrate by *Leuconostoc mesenteroides* subsp *cremoris*. Appl Microbiol Biotechnol 36(5):679–683

Shi Z, Li H, Li Z, Hu J, Zhang H (2013) Pre-column derivatization RP-HPLC determination of amino acids in Asparagi radix before and after heating process. IERI Procedia 5:351–356. https://doi.org/10.1016/j.ieri.2013.11.115

Smid EJ, Erkus O, Spus M, Wolkers-Rooijackers JCM, Alexeeva S, Kleerebezem M (2014) Functional implications of the microbial community structure of undefined mesophilic starter cultures. Microb Cell Fact 13:S2. https://doi.org/10.1186/1475-2859-13-S1-S2

Starrenburg MJC, Hugenholtz J (1991) Citrate fermentation by *Lactococcus* and *Leuconostoc* spp. Appl Environ Microbiol 57(12):3535–3540

Teusink B, van Enckevort FH, Francke C, Wiersma A, Wegkamp A, Smid EJ, Siezen RJ (2005) In silico reconstruction of the metabolic pathways of *Lactobacillus plantarum*: comparing predictions of nutrient requirements with those from growth experiments. Appl Environ Microbiol 71(11):7253–7262. https://doi.org/10.1128/AEM.71.11.7253-7262.2005

Teusink B, Wiersma A, Molenaar D, Francke C, de Vos WM, Siezen RJ, Smid EJ (2006) Analysis of growth of *Lactobacillus plantarum* WCFS1 on a complex medium using a genome-scale metabolic model. J Biol Chem 281(52):40041–40048. https://doi.org/10.1074/jbc.M606263200

Tracey RP, Britz TJ (1989) Cellular fatty-acid composition of *Leuconostoc oenos*. J Appl Bacteriol 66(5):445–456. https://doi.org/10.1111/j.1365-2672.1989.tb05114.x

van Mastrigt O, Abee T, Lillevang SK, Smid EJ (2018) Quantitative physiology and aroma formation of a dairy *Lactococcus lactis* at near-zero growth rates. Food Microbiol 73:216–226. https://doi.org/10.1016/j.fm.2018.01.027

Vinay-Lara E, Hamilton JJ, Stahl B, Broadbent JR, Reed JL, Steele JL (2014) Genome-scale reconstruction of metabolic networks of *Lactobacillus casei* ATCC 334 and 12A. PLoS One 9(11): e110785. https://doi.org/10.1371/journal.pone.0110785

Yi YJ, Lim JM, Gu S, Lee WK, Oh E, Lee SM, Oh BT (2017) Potential use of lactic acid bacteria *Leuconostoc mesenteroides* as a probiotic for the removal of Pb(II) toxicity. J Microbiol 55(4):296–303. https://doi.org/10.1007/s12275-017-6642-x